Soft Matter

PAPER

View Article Online
View Journal | View Issue

Cite this: *Soft Matter*, 2016, 12, 9501

Wrinkle formation in a polymeric drug coating deposited *via* initiated chemical vapor deposition†

Paul Christian,[a] Heike M. A. Ehmann,[bc] Oliver Werzer[bc] and Anna Maria Coclite*[ac]

Received 19th August 2016,
Accepted 7th November 2016

DOI: 10.1039/c6sm01919f

www.rsc.org/softmatter

Polymer encapsulation of drugs is conventionally used as a strategy for controlled delivery and enhanced stability. In this work, a novel encapsulation approach is demonstrated, in which the organic molecule clotrimazole is enclosed into wrinkles of defined sizes. Having defined wrinkles at the drug/encapsulant interface, the contact between the encapsulating polymer and the drug can be improved. In addition, this can also allow for some control on the drug delivery as the available surface area changes with the wrinkle size. For this purpose, thin films of clotrimazole were deposited onto silica substrates and were then encapsulated by crosslinked poly(2-hydroxyethyl methacrylate) (pHEMA) *via* initiated chemical vapor deposition (iCVD). The thickness and the solid state (crystalline or amorphous) of the clotrimazole layer were varied so that the conditions under which surface wrinkles emerge can be determined. A (critical) clotrimazole thickness of 76.6 nm was found necessary to induce wrinkles, whereby the wrinkle size is directly proportional to the thickness of the amorphous clotrimazole. When the pHEMA was deposited on top of crystalline clotrimazole instead, wrinkling was absent. The wrinkling effect can be understood in terms of elastic mismatch between the relatively rigid pHEMA film and the drug layer. In the case of amorphous clotrimazole, the relatively soft drug layer causes a large mismatch resulting in a sufficient driving force for wrinkle formation. Instead, the increased elastic modulus of crystalline clotrimazole reduces the elastic mismatch between drug and polymer, so that wrinkles do not form.

Introduction

Encapsulating drugs with synthetic polymers has several important roles: it creates a diffusion membrane around medications for release in adjustable time-scales;[1,2] it protects the drug during the administration (*e.g.* from acidic environment in the oral route); it enhances the drug stability on storage. This is generally achieved by biocompatible polymer/drug composite layers or by dispersing the drug itself within a soluble or insoluble polymer matrix, thus forming a solid-state dispersion or solution.[3,4]

The recently developed initiated chemical vapor deposition (iCVD) allows the preparation of thin polymer coatings on nearly any surface, including delicate substrates such as liquid layers,[5] paper,[6] organic films[7] or drug molecular layers.[8] iCVD polymerization works in a wide range of environmental conditions, among them mild vacuum and low substrate temperatures, allowing even the direct deposition onto delicate drug formulations which are easily altered by solution-based polymer coating processes.[9] The iCVD process follows the mechanisms of conventional radical polymerization.[10,11] Radicals are created in the vapor phase upon thermal decomposition of an initiator molecule, often a peroxide, by selectively breaking the labile oxygen–oxygen bond at temperatures in the range 250–350 °C. The monomer remains unaffected by these temperatures and gets adsorbed on a substrate held at moderate temperatures (ambient to 60 °C). There, radicals can react with the vinyl bonds of the monomer molecules from the vapor phase, resulting in the formation of heavier initiator–monomer fragments. Subsequently, growth proceeds by attaching additional monomer units to the chain until it is terminated by another radical or unsaturated chain.[12] Further details on this iCVD polymerization mechanism can be found in recent reviews.[9,13]

It has been demonstrated that engineered three-dimensional wrinkles bind the coating intimately to its substrate.[14] When a solid thin film is deposited onto a liquid and forms wrinkles, the liquid seeks to keep the solid–liquid contact by flowing into the wrinkles.[15] In the current study, the encapsulation of a drug molecular layer into a wrinkled, hydrogel-forming layer is investigated. This approach can be applicable for morphology-controlled drug-release, as well as for other practical purposes, including tunability of adhesion,[16,17] wettability[18,19] for microfluidics[20] or optical coatings (anti-reflection layers). In particular,

[a] *Institute of Solid State Physics, NAWI Graz, Graz University of Technology, 8010 Graz, Austria. E-mail: anna.coclite@tugraz.at*
[b] *Institute of Pharmaceutical Science, Department of Pharmaceutical Technology, University of Graz, 8010 Graz, Austria*
[c] *BioTechMed, Graz, Austria*

† Electronic supplementary information (ESI) available: FT-IR spectrum of the pHEMA film, AFM micrographs for the 200 nm pHEMA film on different scales. See DOI: 10.1039/c6sm01919f

keeping the surface chemistry unchanged while varying the morphology in a controlled manner can be beneficial for studies of properties like wettability or crystal growth as a function of the interface morphology. Among three-dimensional surface morphologies, wrinkled surfaces have recently attracted a great deal of attention. Since Bowden's experiments in 1998,[21] many groups have investigated different routes to prepare defined surface wrinkles, both from the experimental and the theoretical point of view. Most often, wrinkles on a surface are obtained when a compressive stress is generated between a coating layer and a substrate due to the expansion mismatch of the two materials.[22]

Ordered wrinkling has already been demonstrated by the deposition of a cross-linked poly(2-hydroxyethyl methacrylate) (pHEMA) layer onto PDMS substrates by iCVD.[23] This resulted in the formation of two-dimensional herringbone patterns by the sequential release of the biaxially stretched PDMS. In this current work, another approach is demonstrated to fabricate wrinkles of various sizes. For this, clotrimazole was encapsulated by crosslinked pHEMA *via* iCVD. Clotrimazole is commonly used in the treatment of fungal disease,[24] but is also evaluated for therapies of malaria.[25] In this study, clotrimazole is used as a model substance as it is stable under mild vacuum conditions (required in our iCVD process) and remains amorphous at a solid substrate for a prolonged period prior and after fabrications, in contrast to other molecules which rapidly transit to a more stable crystalline form.[26] Furthermore, its excellent solubility in organic solvents allows simple but defined film preparation by spin coating. Various films of different thicknesses were prepared, functioning effectively as a spacing layer between the iCVD pHEMA coatings and the rigid silicon substrate, as depicted in Scheme 1. The pHEMA polymer belongs to the category of hydrogels, as it shows a fast response to wet environments. The presence of absorbed water in the polymer network induces a reversible change in thickness from unswollen to the swollen state and *vice versa*. Encapsulating clotrimazole in a pHEMA hydrogel presumably enables the polymer coating to act as diffusion barrier in the dry, unswollen state while allowing for a drug delivery when swollen. For this, also the biocompatibility of pHEMA, which was demonstrated already in several cases, plays an important role.[27,28] In this work, the impact of the drug layer thickness and of its solid state (*i.e.* crystalline *vs.* amorphous) on the wrinkling process was studied. Many studies on wrinkles are based on depositing a hard skin layer on soft substrate and varying the thickness of the skin layer.[29–31] When the skin layer is thick enough, wrinkles form as a result of the elastic mismatch between the rigid film and the soft substrate.[32] In this work, a different approach was chosen: the thickness and the solid state of the clotrimazole layer were varied in order to control wrinkle formation (Scheme 1).

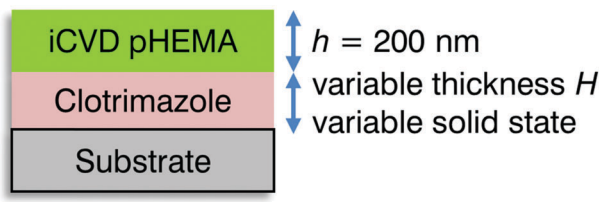

Scheme 1 Schematic of the sample structure, indicating the variables (thickness and solid state of the clotrimazole layer) whose impact on the wrinkling process is evaluated.

Materials and methods

Pharmaceutical grade clotrimazole was purchase from Gatt-Koller GmbH (Austria) and used without further treatment. Tetrahydrofuran (THF) of spectrophotometric grade was purchased from Sigma-Aldrich (Germany). Solutions of clotrimazole in THF were prepared in various solute concentrations, ranging from 1.7 mg g^{-1} to 66.6 mg g^{-1}, and stirred prior usage. Silicon wafers with defined thermally grown oxide of 150 nm (Siegert Wafers, Germany) were used as substrates. Prior usage, the substrates were cleaned by ten minutes sonication each in acetone and ethanol solution, respectively, rinsed with MilliQ water and finally dried under a nitrogen stream.

Defined clotrimazole layers were prepared by spin coating from the different concentrations using a standard spin coating device (Ingenieurbüro Reinmuth, Germany). The spin time was set to 30 seconds at a rotation speed of 25 rounds per second. The clotrimazole layer thicknesses were determined by variable angle spectroscopic ellipsometry using a M-2000 ellipsometer (J. A. Woollam, USA). For the layer thickness extraction, the data was modeled as a system consisting of three-layers including bulk silicon, silicon oxide (150 nm) and clotrimazole, using the CompleteEASE software. The optical constants of the silicon crystal and the surface oxide were taken from literature,[33] while the refractive index of the clotrimazole layer were modeled by a Cauchy function.

iCVD layers were deposited using a custom build setup. The samples were housed in a cylindrical vacuum chamber equipped with a throttle valve, controlling the operating pressure to 350 mTorr. The substrate temperature was kept at 30 ± 3 °C by a chiller/heater system (Thermo Scientific Accel 500 LC). The thermal decomposition of the initiator was induced by a filament array of nickel–chromium wires (Goodfellow, UK), heated to 320 ± 5 °C. The hydrophilic monomer 2-hydroxyethyl methacrylate (HEMA, 97%, Aldrich, Germany), the cross-linking agent ethylene glycol dimethacrylate (EGDMA, 98%, Aldrich, Germany) and the initiator *tert*-butyl peroxide (TBPO, 98%, Aldrich, Germany) were used without further treatment. The two monomers were kept at 75 and 80 °C, respectively, and flown into the reactor through a heated mixing line. The flow rates were adjusted *via* needle valves. The initiator was kept at ambient temperature and was introduced separately into the chamber. The various samples were coated at constant flow rates: TPBO 0.80 ± 0.02 sccm, HEMA 0.75 ± 0.05 sccm, EGDMA 0.04 ± 0.01 sccm and N_2 3.0 ± 0.1 sccm. The N_2 was used as patch flow. A nominal layer thickness of 200 nm was deposited on all the samples, monitored *in situ* by laser interferometry (He–Ne Laser with λ = 633 nm, Thorlabs, USA). Simultaneous to the deposition of clotrimazole layers, also pristine silicon substrates were coated with cross-linked pHEMA to allow for an easier characterization of the polymer properties.

The chemical composition and structure of the pHEMA layer were evaluated by Fourier transform infrared (FT-IR) spectroscopy (Bruker IFS 66 v/S) in transmission. The atomic composition of the compound (clotrimazole and polymer) and the pristine polymers were determined by X-ray photoelectron spectroscopy (XPS). The spectra were acquired using non-monochromatic Mg K-alpha radiation (1253 eV). The pass energy was 50 eV for survey scans and 20 eV for high resolution scans. The take-off angle was 55°. The analysis of the data were performed using Casa XPS. Morphological studies were conducted by a FlexAFM (Nanosurf, Switzerland) using an EasyScan 2 AFM controller and a Tap190 cantilever (BudgetSensors, Bulgaria). The measurements were performed in non-contact mode so that the amplitude of the cantilever, exited at 190 kHz, was used as the feedback loop parameter. The individual images were corrected for sample flatness and artefacts with the software package Gwyddion.[34]

Results and discussion

Amorphous clotrimazole layers on silicon oxide

The deposition of clotrimazole from THF solutions resulted in homogenous films for solute concentrations (c) ranging from 1.7 mg g^{-1} to 66.6 mg g^{-1}. Atomic force microscopy measurements of such films featured little to no surface structures, which is also reflected by a surface roughness (root mean squared, RMS) below 0.4 nm (data not shown). As a previous study has shown, this preparation route generally results in (initially) amorphous clotrimazole films, which is also indicated by the absence of a significant surface roughness.[35]

At solute concentrations lower than 1.7 mg ml^{-1}, holes started to appear in the spin coated clotrimazole layers as the system had not enough time to form a coherent film or the amount of material is not sufficient for covering the entire sample. Exceeding c = 66.6 mg ml^{-1}, the film quality decreased quickly due to comet structure formation by residual particles of un-dissolved clotrimazole in solution, making the surface inhomogeneous. Therefore, only samples in the concentration range of 1.7–66.6 mg ml^{-1} were studied further. Using a different solvent and/or spin coating conditions, crucial parameters such as solubility and evaporation speed can likely be altered, probably pushing the limits for high quality films to thinner but also to thicker ones.

Ellipsometric measurements of the clotrimazole layers show a variation in layer thickness, ranging from 19 nm to 531 nm as the solute concentration is varied from 1.7 to 66.6 mg g^{-1} in the spin coating process (see Fig. 1). The thicknesses in between those two extremes increase linearly with the clotrimazole concentration. A linear regression fit shows that the layer thickness (H) can be described by H [nm] $\sim$ 12.6 + 7.9·c.

When stored under ambient conditions after film fabrication, the appearance and thus the solid state of such films remained unaffected for several hours. This stability allows the subsequent deposition and characterization of polymeric iCVD coatings on top of the amorphous clotrimazole films without the need for other process steps, like heat treatment.

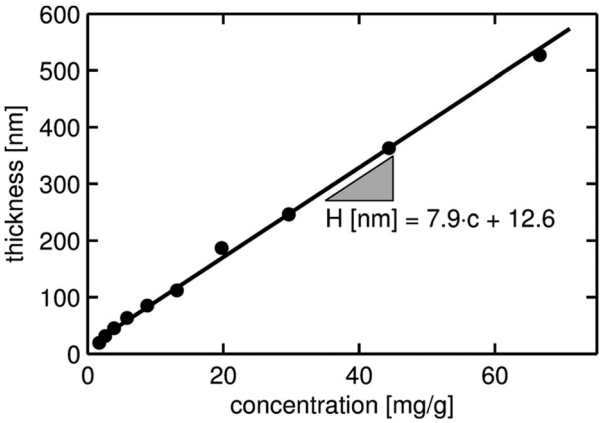

Fig. 1 Layer thicknesses (H) of the clotrimazole films deposited *via* spin coating from various THF solutions. The thickness has been obtained from ellipsometric measurements.

Characterization of the pristine iCVD pHEMA layer

A crosslinked pHEMA hydrogel was deposited onto a silicon oxide surface by iCVD to analyze the layer properties in the absence of clotrimazole. The ratio of monomer to saturation vapor pressure at the substrate surface can be calculated from the deposition parameters, which yields a HEMA to EGDMA ratio of 2 : 1. The film thickness is determined to 206 nm from the ellipsometry data, with the AFM height image showing a homogenous surface with a roughness of 1.2 nm (see Fig. 2, top left). Even if this value is larger than the one of bare silicon oxide surfaces (below 0.3 nm), it is comparable to the typical roughness of solution cast polymer films. This demonstrates that the iCVD process can be utilized to alter the chemical composition of a rigid surface while leaving the roughness (almost) unchanged.

FT-IR measurements were performed to determine the chemical composition of the hydrogel. The FT-IR spectra (ESI,† Fig. S1) show peaks characteristic for both EGDMA and HEMA monomers: the carbonyl ester absorption (1705–1740 cm^{-1}), the methyl and methylene absorption at 2950–2800 cm^{-1} and 1200–1000 cm^{-1} and C–O absorption (1050–1150 cm^{-1}). The characteristic OH band, attributable to the HEMA monomer, is also visible at 3500–3000 cm^{-1}. A detailed analysis of the line profile suggests a crosslinker content, *i.e.* EGDMA content, of (15 $\pm$ 1)%, which is in good agreement with the XPS data of the film. The atomic ratio of carbon-to-oxygen calculated from the XPS spectrum was 2.09 : 1, while a ratio of 2.08 : 1 would be expected from the FTIR data. As the sampling depth in XPS experiments is just about 10 nm and the FT-IR samples instead the whole thickness, the good agreement of the C/O ratios determined by these two techniques hints at a very similar bulk and surface composition. Often, a preferential orientation of apolar groups (*e.g.* methyl groups) at the polymer–air interface or some surface contamination will result in a carbon-enriched surface composition relative to the bulk. In addition, both techniques, *i.e.* FT-IR and XPS analysis, confirm the retention of the monomeric units of HEMA and EGDMA after the deposition as well as a defined copolymer composition.

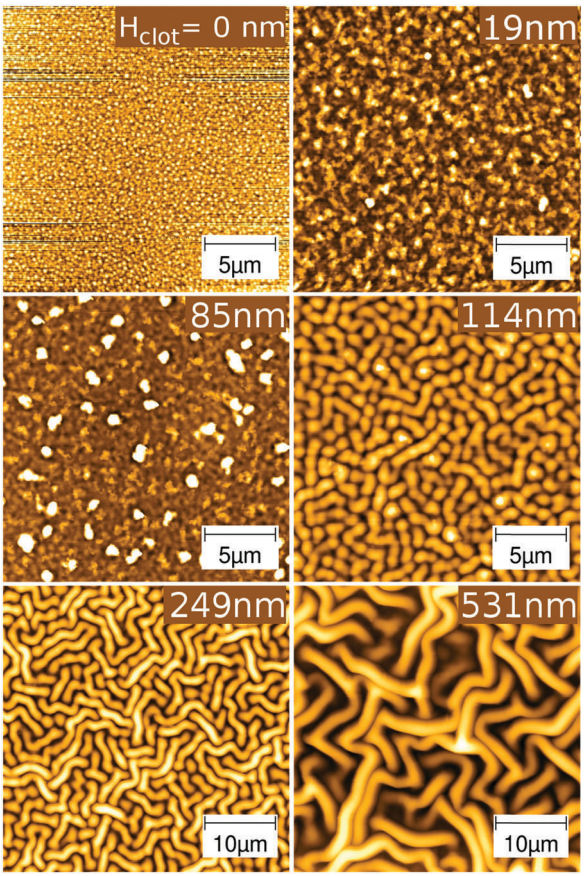

Fig. 2 AFM height images of pHEMA films (h = 206 nm) coated on top of clotrimazole spacing layers of varying thicknesses H, as reported in the labels. For comparison, a pHEMA film on the bare silicon oxide substrate is also shown (label "0 nm"). Note that the color scale and the resolution are different for the individual images, as the feature height varies from a few nanometers to microns.

iCVD coatings on amorphous clotrimazole

The deposition of a crosslinked pHEMA layer onto a rigid bare substrate by the iCVD process resulted in a smooth surface, with the film adhering to the morphology of the substrate. However, when the crosslinked pHEMA is deposited on a relatively soft layer, *i.e.* on top of amorphous clotrimazole (which acts then as a spacing layer from the actual silicon substrate), the morphology drastically changes (see Fig. 2 for selected examples, the complete AFM data are provide in the ESI,† Fig. S2 and S3).

Already at a clotrimazole layer thickness of 19 nm, the deposition of pHEMA resulted in a significant increase in surface roughness (σ_{rms} = 7 nm) when compared to either the bare silicon substrate (23 times), the amorphous clotrimazole (18 times) or the pristine pHEMA film on the silicon wafer (6 times). This means that the growth of the pHEMA layer is affected by the presence of the drug spacing layer underneath even when it is just 19 nm thick.

Increasing the thickness of the clotrimazole spacer slightly did not change the film morphology significantly, indeed the roughness of the iCVD surface on top of a 63 nm thick clotrimazole layer was only σ_{rms} = 9 nm, slightly higher than that of thinner spacers. At a spacer thickness of 85 nm, some dots, bigger than other surface areas, are visible. The number of these dots increases with the thickness of the spacing layer (see ESI†) and reaches a maximum at 85 nm.

At spacer thickness of 114 nm, a transition from the relatively smooth surface morphologies (except for some dots) to surface wrinkles occurs. Many structures appear dot-like but the structure size being significantly larger when compared to the samples containing thinner drug layers. Besides this, structures with elongated shape but of same width and height as the dot-like structures are observed. The length of these can, however, extend several tens of micrometers. In Fig. 2, it can be seen that a further increase in spacer thickness results in much larger structures with mostly fibrillar shape instead of the dot-like one. The thickest sample tested, *i.e.* with a spacer thickness of 531 nm, contains only fibrillar structures, which form a labyrinth-like pattern (Fig. 2). A preferred orientation of the wrinkles is not observed which is expected as neither the underlying isotropic silicon oxide layer nor the amorphous clotrimazole layer introduces any directional surface properties.

To gain further information, the surface root mean square roughnesses (σ_{rms}) of the various samples were extracted from the AFM height images and the results are summarized in Fig. 3. The root mean square roughness values represent the deviation from an average (calculated) surface. This means that σ_{rms} is a good approximation for the peak-to-peak amplitude, *i.e.* the total variation in structure height. For a spacer thickness below 85 nm, the roughness is nearly independent from the thickness of the clotrimazole layer and consequently, the slope of a linear regression fit is close to zero in this region. For spacer thicknesses larger than 85 nm, the roughness drastically changes with the thickness. The increase in roughness is directly proportional to the spacer thickness, with a slope of 1.18. A critical thickness (H_c) can be identified at 79 nm, where the extrapolations of the two linear regressions intercept, *i.e.* for values below H_c, the surface roughness is not (or only little) dependent on the spacer thickness while above, the roughness

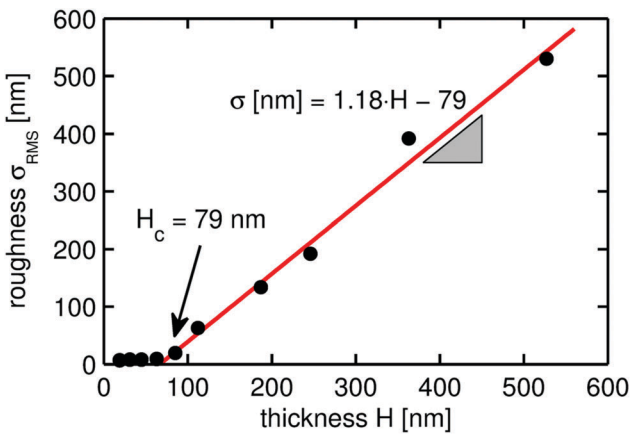

Fig. 3 Root-mean-square roughness of the crosslinked pHEMA surfaces deposited on top of amorphous clotrimazole layers of different thicknesses. The values are calculated from the AFM data presented in Fig. S2 (ESI†).

is a function of the distance between the supporting substrate surface and the pHEMA layer. Huang *et al.* reported such a behavior in a similar study.[15] They observed that there is a critical thickness at which interfacial forces and surface stresses assume a dominant role in the appearance of the surface morphology. Below the critical thickness of the spacing layer, the rigidity of the solid film stabilizes the flat morphology against the wrinkled one. Above the critical thickness, the compressive stress acts on the solid film, inducing wrinkling.

Besides the wrinkling amplitude represented by the roughness parameter, the wavelength is a key parameter of such surface wrinkles. Due to the unordered nature of the wrinkling, the radial power spectral density (RPSD) of the AFM micrographs was used in the determination of the characteristic wrinkle wavelengths. The RPSD is the Fourier transform of the radial autocorrelation function, which represents the power of the spatial frequencies and can thus be utilized to reveal periodic structures on a surface. This evaluation provides only reasonable numbers for samples exhibiting some periodicity (*i.e.* wrinkles), so only data with a spacer thickness of 114 nm and above are considered. At clotrimazole thickness of 114 nm, the wrinkle wavelength is approximately 1100 nm, showing a steady increase up to a maximum of ≈3000 nm as the spacing layer thickness reaches 531 nm.

There are many studies describing and modeling the appearance of wrinkles and relating their characteristics (*e.g.* amplitude, wavelength) to some physically meaningful parameters. Having a multilayer system, a strain relaxation causes wrinkle formation when the individual layers differ in their elastic response (elastic modulus or Young's modulus), whereby most often systems containing a soft substrate (E_s) and a thin, rigid top layer (E_f) are studied.[36]

Then the wrinkle wavelength λ can be related to

$$\lambda = 2\pi h\left(\frac{\bar{E}_f}{3\bar{E}_s}\right)^{1/3}, \quad (1)$$

whereby h denotes the thickness of the clotrimazole film. For the validity of this model, the thickness of the substrate has to be significantly larger than that of the film so that small variations of the substrate thickness (*i.e.* the clotrimazole spacer here) do not influence the forces at the substrate/film interface. However, in the present case, the resulting morphology of the pHEMA thin film is the consequence of the force balance at the polymer–air and the clotrimazole–polymer interface, with the forces at the latter changing with the clotrimazole thickness H. Therefore, assumptions made for the model in eqn (1) are not fulfilled. A model whose assumptions are more similar to our experimental setup regards the case of a stiff film on a compliant substrate of similar thickness.[37] For an incompressible substrate, an analytic expression can be derived:

$$\frac{\lambda}{2\pi h} = \sqrt{\frac{H}{h}}\left(\frac{\bar{E}}{18\bar{E}_s}\right)^{1/6}. \quad (2)$$

The wrinkle wavelength is hereby also a function of the square-root of the substrate to film thickness ratio H/h. This means that from a double logarithmic, normalized plot of the experimental data (*i.e.* λ/h over H/h) the ratio of elastic moduli can be calculated. Eqn (2) represents then a linear function (see Fig. 4) where the intercept with the y-axis corresponds to $\log_{10}\left(2\pi \cdot \left[\frac{\bar{E}}{18\bar{E}_s}\right]^{1/6}\right)$. From this, the elastic modulus ratio of polymer to spacer is derived to 73.

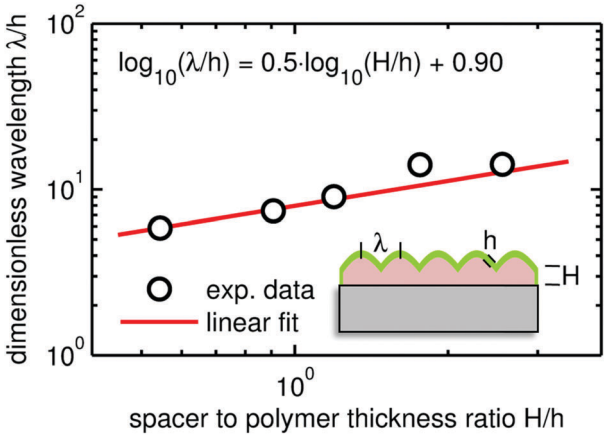

Fig. 4 Wrinkle wavelength represented in a double logarithmic plot, with normalization for the iCVD polymer thickness h. The solid line represents a linear fit of the data, with the corresponding equations given in the inset.

As it is evident from eqn (1) and (2), the wrinkle wavelength is independent of any pre-straining of the substrate before the deposition. Nevertheless, the formation of wrinkles, in general, requires the presence of a compressive stress prior a relaxation step. In most cases, this is achieved by thermal pre-straining of the sample, which results in the wrinkling after stress release/relaxation. In the present case, thermal pre-strain is inherently present as the substrate temperature is above room temperature during deposition. Further, the clotrimazole layer itself has a strong tendency to de-wet the surface, as observed for thinner films. Having thicker films, the de-wetting is balanced by adjacent molecules resulting in a metastable state. A slight disruption of this state might facilitate de-wetting and thus also wrinkle formation.

Encapsulation performance

To obtain an estimate of the encapsulation quality of the pHEMA polymer regarding the ability to protect the clotrimazole layer from the environment, XPS investigations were performed after storing the samples for one month under ambient conditions. In all these measurements, signals from the chlorine unit of the clotrimazole were absent, independently on the spacer thickness. Furthermore, no nitrogen was detected (data not shown). This suggests that the clotrimazole is fully buried below the polymeric layer. From all these measurements it can be concluded that the crosslinked pHEMA layer deposited by iCVD performed well in terms of encapsulating the clotrimazole against ambient.

The results shown here demonstrate also the advantage of using such deposition technique when compared, for instance, with a solution cast technique.[4] In such solution cast films, the

matrix material and the clotrimazole layers formed a solid state solution but the XPS results revealed that a significant amount was hosted at the sample surface. While this may be interesting for a ready drug delivery, the drug molecules are not as well-protected against the environment as in the case of the iCVD encapsulation.

iCVD on partial crystalline film

There are many ways clotrimazole can be transferred into the crystalline state. The method that works fastest without strong de-wetting of the clotrimazole from the substrate is water solvent vapor annealing.[35] Within a couple of days, an initial amorphous film is fully crystallized. In this work, a thick clotrimazole film of 530 nm thickness was stored in water vapor for two days, resulting in the film being partly transferred into a crystalline state. When the iCVD coating was deposited on top of such a partially crystalline film, interesting behaviors were observed in optical and atomic force microscopy images. Firstly, the amorphous fraction of the film contains wrinkles (see Fig. 5a and b). In the vicinity of the crystal, which appears bright in the polarized optical microscopy image, a depletion zone formed, *i.e.* clotrimazole molecules diffuse out of the intermediate region, typically addressed as Ostwald ripening. This depletion region shows a steady increase in thickness, as the distance to either crystalline or amorphous regions is getting smaller (interference due to the layer thickness variation results in the visible color gradient). As a result, also the wrinkling structure deviates in size: the structures are less pronounced for areas containing lower amounts of clotrimazole, in accordance with the findings above.

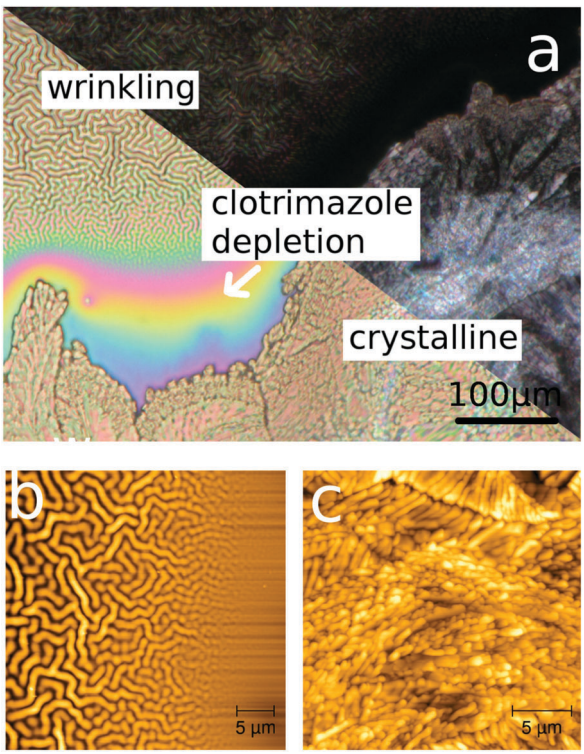

Fig. 5 (a) Optical microscope image of a partial crystalline clotrimazole film coated with a 200 nm pHEMA layer without (lower left triangle) or with (upper right triangle) the usage of a polarizer. AFM height images of areas containing the spacer either in an amorphous (b) or crystalline (c) state.

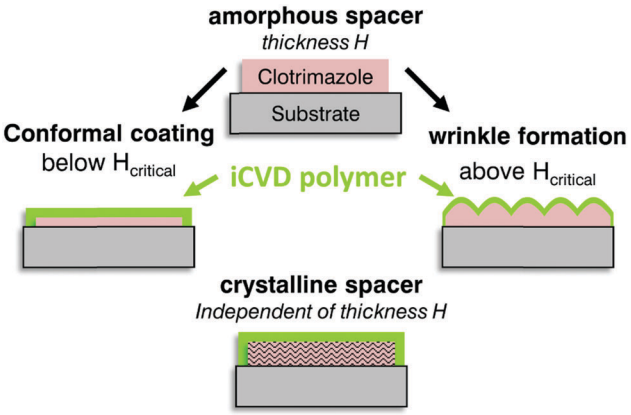

Fig. 6 Scheme of the sample geometry prior iCVD coating and the assembly after deposition on thin or thick amorphous spacer (middle) and on crystalline clotrimazole (bottom).

Having crystalline clotrimazole on the silica surface results in the surface morphology being dominated by the crystal morphology, despite having a pHEMA layer on top. Surface wrinkling does not occur on these surfaces. In the framework of the wrinkling theory described above, this suggests that the elastic response of clotrimazole and polymer are now nearly identical. Such a behavior might be expected as the crystalline state reduces the degrees of freedom, making the system more rigid. As shown elsewhere,[38] wrinkle formation results also for the samples when the crystalline clotrimazole is heated above its melting temperature ($T_m \sim 150$ °C) and subsequently cooled to ambient, since this treatment yields again the amorphous clotrimazole state.

Conclusion

The combination of solution processed drug layers and encapsulation by iCVD polymer depositions promises a highly adaptable and reproducible fabrication process whereby the surface morphology tuning might be of interest to fields beyond the pharmaceutical application. While many methods facilitate different sample compositions and preparation methods, the present approach does not require mechanical pre-stressing or heat treatments. In fact, three different responses in the surface were identified to correlate with the clotrimazole properties being present prior deposition (*cf.* Fig. 6). When the thickness of the clotrimazole/spacer film is below a critical thickness, the iCVD polymer covers the clotrimazole surface with rather conformal layers. Above the critical spacer thickness, the elastic modulus mismatch between the polymer and the drug layer results in strong surface wrinkling. For crystalline spacers, wrinkling is absent and the resulting morphology remains alike the bare crystal surface.

Acknowledgements

The work was funded by the Austrian Science Fund (FWF): [P25541-N19]. The authors want to thank the NAWI Graz for support.

Part of the research was supported by a Marie Curie International Incoming Fellowship (project 626889) within the 7th European Community Framework Programme.

References

1 F. Siepmann, J. Siepmann, M. Walther, R. J. MacRae and R. Bodmeier, Polymer Blends for Controlled Release Coatings, *J. Controlled Release*, 2008, **125**(1), 1–15.
2 J. Siepmann and F. Siepmann, Stability of Aqueous Polymeric Controlled Release Film Coatings, *Int. J. Pharm.*, 2013, **457**(2), 437–445.
3 S. Schrank, B. Kann, E. Saurugger, H. Ehmann, O. Werzer, M. Windbergs, B. J. Glasser, A. Zimmer, J. Khinast and E. Roblegg, Impact of Drying on Solid State Modifications and Drug Distribution in Ibuprofen-Loaded Calcium Stearate Pellets, *Mol. Pharmaceutics*, 2014, **11**(2), 599–609.
4 H. M. A. Ehmann, S. Winter, T. Griesser, R. Keimel, S. Schrank, A. Zimmer and O. Werzer, Dissolution Testing of Hardly Soluble Materials by Surface Sensitive Techniques: Clotrimazole from an Insoluble Matrix, *Pharm. Res.*, 2014, **31**(10), 2708–2715.
5 L. C. Bradley and M. Gupta, Encapsulation of Ionic Liquids within Polymer Shells *via* Vapor Phase Deposition, *Langmuir*, 2012, **28**(27), 10276–10280.
6 K. K. S. Lau, Y. Mao, H. G. Pryce Lewis, S. K. Murthy, B. D. Olsen, L. S. Loo and K. K. Gleason, Polymeric Nanocoatings by Hot-Wire Chemical Vapor Deposition (HWCVD), *Thin Solid Films*, 2006, **501**(1–2), 211–215.
7 N. Chen, P. Kovacik, R. M. Howden, X. Wang, S. Lee and K. K. Gleason, Low Substrate Temperature Encapsulation for Flexible Electrodes and Organic Photovoltaics, *Adv. Energy Mater.*, 2015, **5**(6), 1401442.
8 K. K. S. Lau and K. K. Gleason, All-Dry Synthesis and Coating of Methacrylic Acid Copolymers for Controlled Release, *Macromol. Biosci.*, 2007, **7**(4), 429–434.
9 A. M. Coclite, R. M. Howden, D. C. Borrelli, C. D. Petruczok, R. Yang, J. L. Yagüe, A. Ugur, N. Chen, S. Lee and W. J. Jo, *et al.*, 25th Anniversary Article: CVD Polymers: A New Paradigm for Surface Modification and Device Fabrication, *Adv. Mater.*, 2013, **25**(38), 5392–5423.
10 K. K. S. Lau and K. K. Gleason, Initiated Chemical Vapor Deposition (iCVD) of Poly(alkyl Acrylates): An Experimental Study, *Macromolecules*, 2006, **39**(10), 3688–3694.
11 K. K. S. Lau and K. K. Gleason, Initiated Chemical Vapor Deposition (iCVD) of Poly(alkyl Acrylates): A Kinetic Model, *Macromolecules*, 2006, **39**(10), 3695–3703.
12 S. H. Baxamusa and K. K. Gleason, Thin Polymer Films with High Step Coverage in Microtrenches by Initiated CVD, *Chem. Vap. Deposition*, 2008, **14**(9–10), 313–318.
13 B. Reeja-Jayan, P. Kovacik, R. Yang, H. Sojoudi, A. Ugur, D. H. Kim, C. D. Petruczok, X. Wang, A. Liu and K. K. Gleason, A Route Towards Sustainability Through Engineered Polymeric Interfaces, *Adv. Mater. Interfaces*, 2014, **1**(4), 1400117.
14 L. R. J. Scarratt, B. S. Hoatson, E. S. Wood, B. S. Hawkett and C. Neto, Durable Superhydrophobic Surfaces *via* Spontaneous Wrinkling of Teflon AF, *ACS Appl. Mater. Interfaces*, 2016, **8**(10), 6743–6750.
15 R. Huang and Z. Suo, Very Thin Solid-on-Liquid Structures: the Interplay of Flexural Rigidity, Membrane Force, and Interfacial Force, *Thin Solid Films*, 2003, **429**(1–2), 273–281.
16 E. P. Chan, E. J. Smith, R. C. Hayward and A. J. Crosby, Surface Wrinkles for Smart Adhesion, *Adv. Mater.*, 2008, **20**(4), 711–716.
17 S. Vajpayee, K. Khare, S. Yang, C.-Y. Hui and A. Jagota, Adhesion Selectivity Using Rippled Surfaces, *Adv. Funct. Mater.*, 2011, **21**(3), 547–555.
18 S. Yang, K. Khare and P.-C. Lin, Harnessing Surface Wrinkle Patterns in Soft Matter, *Adv. Funct. Mater.*, 2010, **20**(16), 2550–2564.
19 C. Bukowsky, J. M. Torres and B. D. Vogt, Slip-Stick Wetting and Large Contact Angle Hysteresis on Wrinkled Surfaces, *J. Colloid Interface Sci.*, 2011, **354**(2), 825–831.
20 T. Ohzono, H. Monobe, K. Shiokawa, M. Fujiwara and Y. Shimizu, Shaping Liquid on a Micrometre Scale Using Microwrinkles as Deformable Open Channel Capillaries, *Soft Matter*, 2009, **5**(23), 4658–4664.
21 N. Bowden, S. Brittain, A. G. Evans, J. W. Hutchinson and G. M. Whitesides, Spontaneous Formation of Ordered Structures in Thin Films of Metals Supported on an Elastomeric Polymer, *Nature*, 1998, **393**(6681), 146–149.
22 G. Gioia and M. Ortiz, Delamination of Compressed Thin Films, in *Advances in Applied Mechanics*, ed. J. W. Hutchinson and T. Y. Wu, Elsevier, 1997, vol. 33, pp. 119–192.
23 J. Yin, J. L. Yagüe, D. Eggenspieler, K. K. Gleason and M. C. Boyce, Deterministic Order in Surface Micro-Topologies through Sequential Wrinkling, *Adv. Mater.*, 2012, **24**(40), 5441–5446.
24 P. R. Sawyer, R. N. Brogden, K. M. Pinder, T. M. Speight and G. S. Avery, Clotrimazole: A Review of Its Antifungal Activity and Therapeutic Efficacy, *Drugs*, 1975, **9**(6), 424–447.
25 V. Borhade, S. Pathak, S. Sharma and V. Patravale, Clotrimazole Nanoemulsion for Malaria Chemotherapy. Part I: Preformulation Studies, Formulation Design and Physicochemical Evaluation, *Int. J. Pharm.*, 2012, **431**(1–2), 138–148.
26 H. M. A. Ehmann and O. Werzer, Surface Mediated Structures: Stabilization of Metastable Polymorphs on the Example of Paracetamol, *Cryst. Growth Des.*, 2014, **14**(8), 3680–3684.
27 R. K. Bose and K. K. S. Lau, Initiated CVD of Poly-(2-Hydroxyethyl Methacrylate) Hydrogels: Synthesis, Characterization and In-Vitro Biocompatibility, *Chem. Vap. Deposition*, 2009, **15**(4–6), 150–155.
28 G.-H. Hsiue, J.-A. Guu and C.-C. Cheng, Poly(2-Hydroxyethyl Methacrylate) Film as a Drug Delivery System for Pilocarpine, *Biomaterials*, 2001, **22**(13), 1763–1769.
29 N. Bowden, W. T. S. Huck, K. E. Paul and G. M. Whitesides, The Controlled Formation of Ordered, Sinusoidal Structures by Plasma Oxidation of an Elastomeric Polymer, *Appl. Phys. Lett.*, 1999, **75**(17), 2557–2559.
30 C. M. Stafford, C. Harrison, K. L. Beers, A. Karim, E. J. Amis, M. R. VanLandingham, H.-C. Kim, W. Volksen, R. D. Miller

and E. E. Simonyi, A Buckling-Based Metrology for Measuring the Elastic Moduli of Polymeric Thin Films, *Nat. Mater.*, 2004, **3**(8), 545–550.

31 E. P. Chan and A. J. Crosby, Spontaneous Formation of Stable Aligned Wrinkling Patterns, *Soft Matter*, 2006, **2**(4), 324–328.

32 J. Genzer and J. Groenewold, Soft Matter with Hard Skin: From Skin Wrinkles to Templating and Material Characterization, *Soft Matter*, 2006, **2**(4), 310–323.

33 C. M. Herzinger, B. Johs, W. A. McGahan, J. A. Woollam and W. Paulson, Ellipsometric Determination of Optical Constants for Silicon and Thermally Grown Silicon Dioxide *via* a Multi-Sample, Multi-Wavelength, Multi-Angle Investigation, *J. Appl. Phys.*, 1998, **83**(6), 3323–3336.

34 D. Nečas and P. Klapetek, Gwyddion: An Open-Source Software for SPM Data Analysis, *Cent. Eur. J. Phys.*, 2011, **10**(1), 181–188.

35 H. M. A. Ehmann, A. Zimmer, E. Roblegg and O. Werzer, Morphologies in Solvent-Annealed Clotrimazole Thin Films Explained by Hansen-Solubility Parameters, *Cryst. Growth Des.*, 2014, **14**(3), 1386–1391.

36 E. Cerda and L. Mahadevan, Geometry and Physics of Wrinkling, *Phys. Rev. Lett.*, 2003, **90**(7), 74302.

37 Z. Y. Huang, W. Hong and Z. Suo, Nonlinear Analyses of Wrinkles in a Film Bonded to a Compliant Substrate, *J. Mech. Phys. Solids*, 2005, **53**(9), 2101–2118.

38 P. Christian, H. M. A. Ehmann, A. M. Coclite and O. Werzer, Polymer Encapsulation of an Amorphous Pharmaceutical by Initiated Chemical Vapor Deposition for Enhanced Stability, *ACS Appl. Mater. Interfaces*, 2016, **8**, 21177–21184.

